Exploring Possible Triangle Singularities in the $\Xi_b^- \to K^- J/\psi \Lambda$ Decay

Chao-Wei Shen [1],* , **Hao-Jie Jing** [1,2] , **Feng-Kun Guo** [1,2] and **Jia-Jun Wu** [1]

1 School of Physical Sciences, University of Chinese Academy of Sciences, Beijing 100049, China; jinghaojie@itp.ac.cn (H.-J.J.); fkguo@itp.ac.cn (F.-K.G.); wujiajun@ucas.ac.cn (J.-J.W.)
2 CAS Key Laboratory of Theoretical Physics, Institute of Theoretical Physics, Chinese Academy of Sciences, Beijing 100190, China
* Correspondence: shencw@ucas.ac.cn

Abstract: We analyze possible singularities in the $J/\psi \Lambda$ invariant mass distribution of the $\Xi_b^- \to K^- J/\psi \Lambda$ process via triangle loop diagrams. Triangle singularities in the physical region are found in 18 different triangle loop diagrams. Among those with Ξ^*-charmonium-Λ intermediate states, the one from the $\chi_{c1}\Xi(2120)\Lambda$ loop, which is located around 4628 MeV, is found the most likely to cause observable effects. One needs S- and P-waves in $\chi_{c1}\Lambda$ and $J/\psi \Lambda$ systems, respectively, when the quantum numbers of these systems are $1/2^+$ or $3/2^+$. When the quantum numbers of the $\Xi(2120)$ are $J^P = 1/2^+, 1/2^-$ or $3/2^+$, the peak structure should be sharper than the other J^P choices. This suggests that although the whole strength is unknown, we should pay attention to the contributions from the Ξ^*-charmonium-Λ triangle diagram if structures are observed in the $J/\psi \Lambda$ invariant mass spectrum experimentally. In addition, a few triangle diagrams with the $D_{s1}^*(2700)$ as one of the intermediate particles can also produce singularities in the $J/\psi \Lambda$ distribution, but at higher energies above 4.9 GeV.

Keywords: triangle singularity; pentaquarks; exotic hadrons

1. Introduction

In the earliest prediction of the hidden-charm baryon $N_{c\bar{c}}$ states above 4 GeV [1], which are now known as the P_c states and have been reported by the LHCb Collaboration [2,3], the $\Lambda_{c\bar{c}}$ states are also predicted with different masses and spin-parities. Ten $\Lambda_{c\bar{c}}$ states are obtained in a coupled-channel model in Ref. [4] and their couplings to $J/\psi \Lambda$ are found to be sufficiently large. Similar to the discovery of the P_c states in the $J/\psi p$ channel [5], the $\Lambda_{c\bar{c}}$ states could be sought in the $J/\psi \Lambda$ invariant mass distributions. In Ref. [6], ten isoscalar molecular pentaquarks in the $\bar{D}^{(*)}\Xi_c$, $\bar{D}^{(*)}\Xi_c'$ and $\bar{D}^{(*)}\Xi_c^*$ systems are predicted by calculating the effective potentials with the chiral effective field theory up to the next-to-leading order. These hidden-charm pentaquark states with strangeness are investigated in the quark model including the color octet type and color singlet type [7] and the one-boson exchange model [8]. The decay behaviors of the $\Lambda_{c\bar{c}}$ states in various hadronic molecular assumptions with different spin-parities are studied in Ref. [9] and these decay patterns are suggested to help understanding the internal structures after the experimental searches. Although there are various predictions for such strangeness baryons within hidden charm theoretically, there is no experimental evidence for them until now.

Since the first prediction of the $\Lambda_{c\bar{c}}$ states, there arises various suggestions of searching for these states experimentally. The decay of Λ_b into $J/\psi K^0 \Lambda$ states is studied in Ref. [10] and a clear peak is predicted in the $J/\psi \Lambda$ invariant mass distribution. In Ref. [11], the authors propose the $\Lambda_b \to J/\psi \eta \Lambda$ decay and find that a resonance signal with similar strength as the case of P_c should be observed

in the $J/\psi\Lambda$ invariant mass spectrum. The $\Xi_b^- \to J/\psi K^-\Lambda$ reaction is discussed in Ref. [12] and a hidden-charm pentaquark state with strangeness is expected to be clearly seen. In the last process, the K^- meson in the final state is a charged meson, and it makes this process suitable for experimental measurement. Actually, the possible peak structures in the $J/\psi\Lambda$ invariant mass spectrum in the $\Xi_b^- \to J/\psi K^-\Lambda$ decay have already been sought by the LHCb Collaboration [13], while the results of these data should still be under analysis. At this point, it is worthwhile to mention that the $\Lambda_b^0 \to J/\psi\Lambda\pi^+\pi^-$ should also be a promising process to seek for the $\Lambda_{c\bar{c}}$ states. In this paper, we will study the $\Xi_b^- \to K^- J/\psi\Lambda$ decay and focus on another mechanism, triangle singularity, which could also produce peak structures in the $J/\psi\Lambda$ invariant mass spectrum.

A triangle singularity is due to the simultaneous on-shellness of three intermediate particles in a loop diagram, and at the same time the interactions at all vertices can happen classically [14]. It is a logarithmic singularity, and is able to produce peaks in energy distributions. It has been known for a long time [15–17], and there were debates in the 1960s on whether it could produce observable effects [18]. Nevertheless, it was difficult to find reactions that satisfy the rigorous kinematic conditions and at the same time can evade the subtle interfering cancellation between the tree-level and triangle diagram, dictated by the Schmid theorem at that time [18]. In the last 10 years or so, suggestions were proposed that many reactions which can be (or have been) measured at modern high-energy experiments could match the kinematic conditions and might receive important contributions from triangle singularities; then the study of triangle singularity started to bring a lot interest until now [3,19–59]. For a recent review, we refer to Ref. [60] (see Tables 1 and 2 therein for reactions proposed since the 1990s).

The fact that triangle singularities may affect the extraction of the P_c resonance parameters from the $\Lambda_b \to J/\psi K^- p$ reaction was immediately noticed [27,28]. Later, the $\Lambda(1890)\chi_{c1}p$ triangle was identified to be the most special from an analysis of many triangle diagrams with various possible combinations of a a charmonium, a proton and a Λ^* [31]. In this case, both triangle singularity and threshold effect occur at about 4.45 GeV as already pointed out in Ref. [28]. Once the $\chi_{c1}p$ is in an S-wave, such that the quantum numbers of the $J/\psi p$ could be $J^P = 1/2^+$ or $3/2^+$, it would generate a narrow peak in the $J/\psi p$ invariant mass distribution. The updated LHCb measurement [3] does not have a peak at 4.45 GeV, but there is a dip at this energy between the two narrow $P_c(4440)$ and $P_c(4457)$ peaks. Thus, the possibility of interference of such a triangle singularity with pentaquark signals is still there, and might be partly responsible for the special production properties of the P_c states [61]. However, for the cases that the spin and parity of the P_c are $3/2^-$ or $5/2^+$, as considered in, e.g., Refs. [62–68], the triangle singularity contribution from the $\Lambda^*(1890)\chi_{c1}p$ loop would be severely suppressed. In the present work, we will investigate possible triangle singularities in the $\Xi_b^- \to J/\psi K^-\Lambda$ reaction in a similar way to Ref. [31].

This work is organized as follows. After the introduction, we first show the theoretical framework and an analysis of possible triangle singularities in Section 2, and the corresponding discussions are presented. Then in Section 3, a detailed analysis and discussions of the amplitude with $\Xi(2120)\chi_{c1}\Lambda$ are given, which is followed by a brief summary in Section 4.

Table 1. The charmonium and Ξ^{*-} states in Figure 1a that could generate triangle singularities and the positions of the corresponding singularities. Among the listed hyperons, $\Xi(2030)$ is a three-star state; $\Xi(2250)$ and $\Xi(2370)$ are two-star states; $\Xi(2120)$ and $\Xi(2500)$ are one-star states [69].

No.	$c\bar{c}$	Ξ^{*-}	Position of Triangle Singularity (MeV)
1	J/ψ	$\Xi(2500)$	4232
2	χ_{c0}	$\Xi(2250)$	4546
3	χ_{c0}	$\Xi(2370)$	4665
4	χ_{c1}	$\Xi(2120)$	4628
5	χ_{c1}	$\Xi(2250)$	4696
6	χ_{c2}	$\Xi(2120)$	4680
7	h_c	$\Xi(2120)$	4644
8	h_c	$\Xi(2250)$	4730
9	$\eta_c(2S)$	$\Xi(2030)$	4754
10	$\eta_c(2S)$	$\Xi(2120)$	4797
11	$\psi(2S)$	$\Xi(2030)$	4810

Table 2. The D_s^{*-}, Ξ_c^{*0} and intermediate particle 3 in Figure 1b,c that could generate triangle singularities and the positions of the corresponding singularities.

No.	D_s^{*-}	Ξ_c^{*0}	Intermediate Particle 3	Position of Triangle Singularity (MeV)
1	$\bar{D}_{s1/s3}^*(2860)$	$\Xi_c(2930)$	$\bar{D}^0$	4838
2	$\bar{D}_{s1}^*(2700)$	$\Xi_c(3055)$	$\bar{D}^0$	4922
3	$\bar{D}_{s1}^*(2700)$	$\Xi_c(3080)$	$\bar{D}^0$	4957
4	$\bar{D}_{s1/s3}^*(2860)$	$\Xi_c(2930)$	$\bar{D}^{*0}$	4959
5	$\bar{D}_{s1}^*(2700)$	$\Xi_c(3080)$	$\bar{D}^{*0}$	5089
6	$\bar{D}_{s1}^*(2700)$	$\Xi_c(3080)$	Λ_c^+	4990
7	$\bar{D}_{s1/s3}^*(2860)$	$\Xi_c(2930)$	Λ_c^+	5149

2. Theoretical Framework and Analysis Results of All Possible Triangle Singularities

In the process of a triangle loop diagram, the initial particle first decays to two intermediate particles *A* and *B*. Then particle *A* continues to decay into two particles, one of which is a final state and the other is the intermediate particle *C*. This intermediate particle *C* could interact with particle *B* to generate final state particles. The kinematic conditions for a triangle singularity in the physical region are [18,31]: (1) the three intermediate particles *A*, *B* and *C* are all on the mass shell at the same time; (2) the velocity of particle *C* is larger than that of particle *B* and is in the same direction in the rest frame of the initial state. In other words, triangle singularity corresponds to the situation that the loop reaction has actually occurred as a classical process [14], rather than a virtual process. We are interested in the possible triangle singularity effects in the $J/\psi\Lambda$ invariant mass distribution. The region of triangle singularity peak is limited to a small region starting from the threshold of two particles that rescatter into the final-state $J/\psi\Lambda$ (for a detailed analysis, see Ref. [60]).

There are four possible kinds of triangle diagrams for the $\Xi_b^- \to K^-\Lambda J/\psi$ decay that may have a triangle singularity in the physical region (when the widths of the intermediate particles are neglected) as shown in Figure 1. Using the intuitive equation derived in Ref. [31], we find that the physical-region triangle singularity emerges in the process of Figure 1a–c.

The Ξ^{*-} in Figure 1a represents all the ten Ξ resonances in the Review of Particle Physics (RPP) [69], including $\Xi(1530)$, $\Xi(1620)$, $\Xi(1690)$, $\Xi(1820)$, $\Xi(1950)$, $\Xi(2030)$, $\Xi(2120)$, $\Xi(2250)$, $\Xi(2370)$ and $\Xi(2500)$. For the charmonium states $c\bar{c}$, we take η_c, J/ψ, χ_{c0}, χ_{c1}, χ_{c2}, h_c, $\eta_c(2S)$ and $\psi(2S)$ into consideration. We take all the listed Ξ_c^{*0} and D_s^{*-} in RPP [69] into account for the exchanged particles in Figure 1b,c.
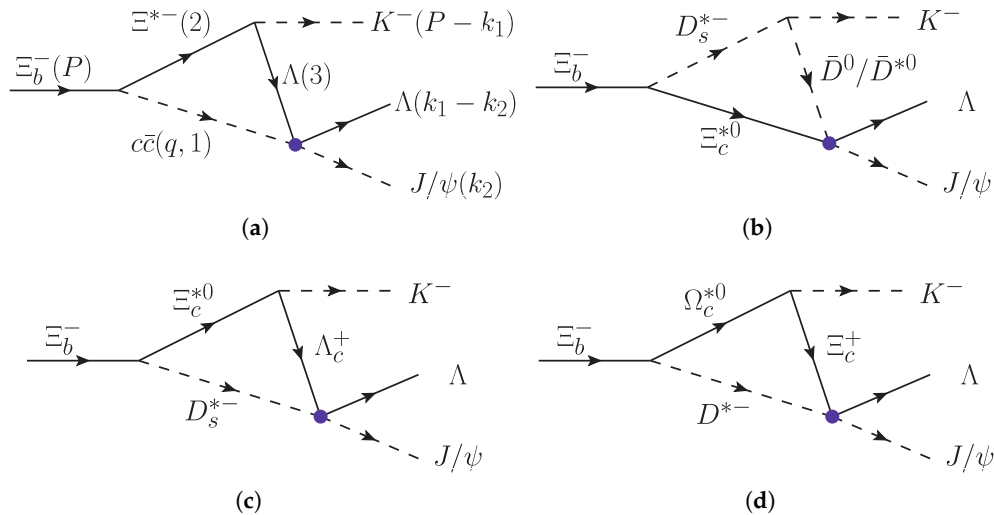
Figure 1. Four possible kinds of triangle diagrams for the $\Xi_b^- \to K^-\Lambda J/\psi$ decay that may have a triangle singularity of interest. The momentum of each particle and the numbering of the exchanged particles used here are given in the brackets in the first diagram.

Through checking the two conditions of triangle singularity for all possible combinations of the considered intermediate particles mentioned above, we find that there are in total 11 cases for Figure 1a and 7 cases for Figure 1b,c that would have singularities in the physical region. The charmonium and Ξ^{*-} states in Figure 1a, which could generate peak structures in the $J/\psi\Lambda$ mass spectrum, and the corresponding positions of these triangle singularities are given in Table 1. In Table 2, we present the three exchanged particles of Figure 1b,c together with the corresponding triangle singularity positions, which are generally higher than those from Figure 1a listed in Table 1. Note that there is another combination, $\bar{D}_{sJ}(3040)\Xi_c(3645)\bar{D}^0$, which can give rise to a triangle singularity at 4511 MeV. However, so far the $D_{sJ}(3040)$ has only been observed in D^*K [69], suggesting that it might have an unnatural parity and thus could not decay into $\bar{D}K$. Consequently, this combination is not listed in the table. One notices that both the $D_{s1}^*(2700)$ was observed in $B \to D\bar{D}K$ [70,71] and the $D_{s1/s3}^*(2860)$ were seen in the decays of $B_s \to \bar{D}\bar{K}\pi$ [72]. Similarly, the $D_{s1}^*(2700)$ should be easily produced from the decays of the Ξ_b associated with a Ξ_c baryon, as shown in the first vertex in Figure 1b,c. Thus, among the combinations listed in Table 2, the ones with the $D_{s1}^*(2700)$ are expected to be more important than the others. Once a structure is observed in the $J/\psi\Lambda$ spectrum above 4.9 GeV in a future experiment, such triangle singularities need to be considered. In the rest of this paper, we will focus on the singularities in Table 1, whose situation is more involved.

Since the triangle singularity is caused by the on-shellness of the intermediate particles, we first consider the scalar loop integral as follows,

$$I = i \int \frac{d^4q}{(2\pi)^4} \frac{1}{(q^2 - m_1^2 + im_1\Gamma_1)[(P-q)^2 - m_2^2 + im_2\Gamma_2][(k_1-q)^2 - m_3^2 + i\epsilon]}, \tag{1}$$

where the momenta and the numbering of particle masses are as given in the first diagram in Figure 1, and Γ_1 and Γ_2 are the widths of intermediate particles 1 and 2, respectively. We can use $|I|^2$ to analyze the singular behavior of the diagrams in Figure 1. It should be noted that the interactions of all the

related vertices are not included here. We should consider these interactions from a physical point of view to draw further conclusions.

Let us turn to the three vertices in Figure 1a. For the first vertex $\Xi_b \to \Xi^* c\bar{c}$, it is a weak decay and involves the Cabibbo–Kobayashi–Maskawa (CKM) matrix elements $V_{bc}^* V_{cs}$. The strength should be comparable with that of $B \to K c\bar{c}$ for the same charmonium. The branching ratios for different charmonia in the latter process, which can be found in the RPP [69], are given in Table 3. It can be seen that for the χ_{c2} and h_c, the branching ratios are one-order-of-magnitude smaller than that of the other charmonia. This indicates that the cases of the charmonium being the χ_{c2} or h_c would not provide a strong signal of triangle singularity, and can be safely neglected. For χ_{c0}, the decay rates from the neutral and charged B mesons are very different. Both the two branching ratios of the χ_{c0} are smaller than the rest, although in the charged case it is of the same order of magnitude. We conclude that, for the $\Xi_b \to \Xi^* c\bar{c}$ decay, the cases where the intermediate charmonium is one of J/ψ, χ_{c1}, $\eta_c(2S)$ and $\psi(2S)$ are expected to be the main decay channels.

Table 3. The branching ratios for different charmonia in $B \to K c\bar{c}$.

$c\bar{c}$	$BR(B^0 \to c\bar{c}K^0)$	$BR(B^+ \to c\bar{c}K^+)$
J/ψ	8.73×10^{-4}	1.01×10^{-3}
χ_{c0}	1.11×10^{-6}	1.49×10^{-4}
χ_{c1}	3.93×10^{-4}	4.84×10^{-4}
χ_{c2}	$<1.5 \times 10^{-5}$	1.1×10^{-5}
h_c		$<3.8 \times 10^{-5}$
$\eta_c(2S)$		4.4×10^{-4}
$\psi(2S)$	5.8×10^{-4}	6.21×10^{-4}

For the vertex of $c\bar{c}\Lambda \to J/\psi\Lambda$, the coupling strength is affected from the spin interactions between the charm quark and anticharm quark. Once the $c\bar{c}$ has a spin flip, this vertex will be much suppressed due to breaking the heavy quark spin symmetry. The quantum numbers of the final state J/ψ are 1^-, and the spins of charm and anticharm quarks are in the same direction. However, in the charmonia h_c and $\eta_c(2S)$, the total spin of charm and anticharm quarks is 0. Therefore, the $h_c\Lambda$ or $\eta_c(2S)\Lambda \to J/\psi\Lambda$ process would be suppressed because of the spin flip of the charm and anticharm quarks. For the other charmonia considered here, the couplings of $c\bar{c}\Lambda \to J/\psi\Lambda$ could be of the same order of magnitude but are still not determined. We will write the amplitudes with different J^P assumptions that are subject to the Lorentz covariant orbital-spin coupling scheme [73] to study their behavior in the next section.

For the $\Xi^*\bar{K}\Lambda$ vertex, we can infer its strength from the $\Xi^* \to \Lambda\bar{K}$ process for each considered Ξ^* state. For the $\Xi(2030)$, the $\Lambda\bar{K}$ state occupies about 20% of all possible decay rates. In the RPP, the $\Lambda\bar{K}$ channel is the only seen and listed decay mode for the $\Xi(2120)$ [69], although its exact ratio has not been measured yet. The $\Lambda\bar{K}$ channel is not listed in the decay modes of the $\Xi(2250)$ and $\Xi(2370)$, and actually all the decay channels for the former are three-body states, meaning that the $\Lambda\bar{K}$ mode might be suppressed for these two states. For the $\Xi(2500)$, the $\Lambda\bar{K}$ mode is listed, with the ratio of branching fractions $\Gamma(\Lambda\bar{K}) / \left(\Gamma(\Xi\pi) + \Gamma(\Lambda\bar{K}) + \Gamma(\Sigma\bar{K}) + \Gamma(\Xi(1530)\pi)\right) = 0.5 \pm 0.2$ measured in Ref. [74], but it is not clear whether the peak observed therein corresponds to the $\Xi(2500)$ as commented in RPP [69].

Through the analysis of the three vertices above, for the 11 cases listed in Table 1, nos. 2 and 3 and nos. 5–10 are suppressed; only nos. 1, 4 and 11 are left. Now let us turn to the character of the intermediate particles in the loop, especially their quantum numbers, since they actually affect a lot not only the magnitude but also the line shape of the singularity. The quantum numbers are quite important as they directly determine the partial waves of the interaction, and high partial wave

interactions should be suppressed in the near-threshold region. For the $\Xi(2030)$ state, its spin is equal to or greater than 5/2 [75]. It leads to high partial-wave ($l \geq 2$) interaction at the $\Xi(2030)\bar{K}\Lambda$ vertex, and will not be considered further. We will discuss that how the high partial-wave interactions in the triangle loop would suppress the contribution of the triangle singularity later. For the other two Ξ^* states, their quantum numbers are not determined yet, and we will consider various J^P possibilities later.

The $m_{J/\psi\Lambda}$ distribution for $|I|^2$ with an arbitrary normalization factor of these three cases is shown in Figure 2. For the widths of the involved charmonium, we quote their central values given in the RPP [69]. While for some of the Ξ^* states like the $\Xi(2120)$ and $\Xi(2500)$, the widths are not precisely determined. For the width of the former, we take the upper bound of the given range, which is 20 MeV. In the latter case, two values were reported by different experimental groups, which are 150 [74] and 59 MeV [76]. We give results using these two values. As shown in Figure 2, the triangle singularity from the $J/\psi\Xi(2500)\Lambda$ loop diagram is much broader than the other two cases. As discussed above, the triangle loop diagram that involves the $\Xi(2030)\bar{K}\Lambda$ vertex should be severely suppressed because of the existence of the D- or higher wave interaction, while for the $\Xi(2120)$ involved vertices, there could be lower partial-wave interactions. The contribution from the $\Xi(2120)\chi_{c1}\Lambda$ loop (the blue dotdashed line in Figure 2) is expected to be much larger than that from the $\Xi(2030)\psi(2S)\Lambda$ (the green dotted line) once all the interactions at the vertices are included.
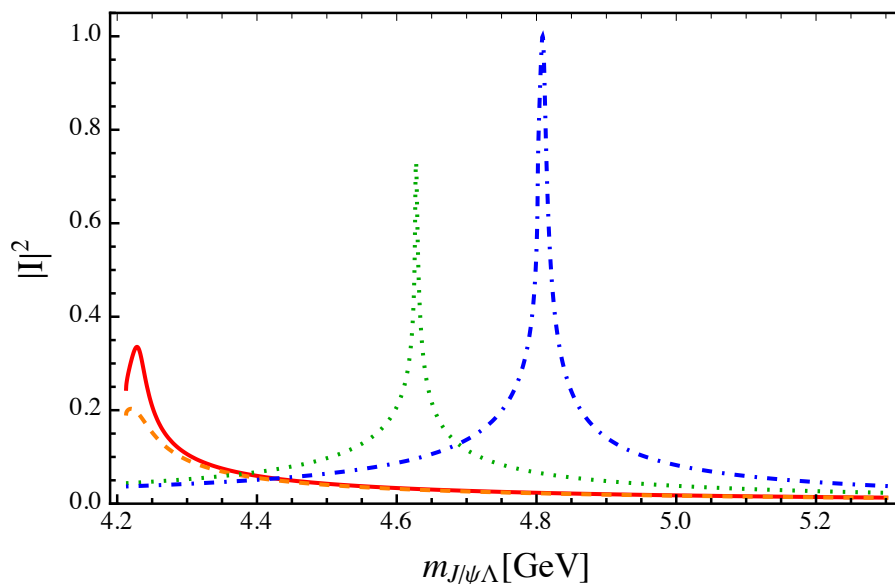
Figure 2. The value of $|I|^2$ in the $m_{J/\psi\Lambda}$ invariant mass distribution. The red solid (orange dashed), green dotted and blue dotdashed lines correspond to the Nos. 1, 4 and 11 cases in Table 1, respectively. For the case of No.1, the red solid and orange dashed lines represent the different choices of the $\Xi(2500)$ width: the narrower and wider peaks correspond to taking 59 and 150 MeV for the width, respectively.

Combining all the analysis above, the $\Xi(2120)\chi_{c1}\Lambda$ loop is found to be the most promising process to generate an observable triangle singularity in the $\Xi_b^- \to K^- J/\psi\Lambda$ decay (We should also note that the $\Xi(2120)$ is just a one-star state [69], and its existence needs further confirmation). We will calculate and discuss the structures from this triangle loop diagram in detail in the next section.

3. Detailed Analysis of the Amplitudes for the Diagram with $\chi_{c1}\Xi(2120)\Lambda$ Loop

We will focus on the triangle diagram involving the χ_{c1} and the $\Xi(2120)$ in this section, as it is the most promising diagram to have a sizeable triangle singularity contribution. The specific interactions of vertices are taken into account in this section, here we are going to study them by constructing effective Lagrangians with the lowest number of derivatives. At present, the quantum numbers of the

$\Xi(2120)$ state and the $J/\psi\Lambda$ system are both flexible, and the former affects the $\Xi_b\Xi^*\chi_{c1}$ and $\Xi^*\Lambda K^-$ vertices, while the later influences the $\chi_{c1}\Lambda J/\psi\Lambda$ vertex. Let us discuss them one by one.

Firstly, let us consider different choices of the spin-parity quantum numbers of the $\Xi(2120)$, which are still unknown. The two vertices involving the $\Xi(2120)$ in this diagram are $\Xi_b\Xi(2120)\chi_{c1}$ and $\Xi(2120)\Lambda\bar{K}$. In Table 4, the assumed spin-parity of $\Xi(2120)$ and the corresponding lowest allowed partial waves of these two vertices are listed. In the Lorentz covariant orbital-spin coupling scheme, the interaction of a vertex is directly related to its partial wave L and the relative momentum of the two final particles, i.e., the strength of interaction is proportional to q^L. Therefore, the D- or higher partial waves are neglected since the momentum is very small around where the triangle singularity happens. Thus, $J^P = 1/2^+, 1/2^-$ and $3/2^+$ possibilities are not suppressed by high partial waves. Among these three cases, the $J^P = 1/2^-$ possibility is singled out as both vertices are in S waves, and the strength of the amplitude in this case should be stronger than that of the other cases. Therefore, we will calculate the amplitude with $J^P(\Xi^*) = 1/2^-$ to check the structure behavior from the triangle singularity.

Table 4. The interactions of the $\Xi_b\Xi(2120)\chi_{c1}$ and $\Xi(2120)\Lambda\bar{K}$ vertices with different spin-parities of $\Xi(2120)$.

J^P	$\Xi_b\Xi(2120)\chi_{c1}$	$\Xi(2120)\Lambda\bar{K}$
$1/2^+$	*S*-wave	*P*-wave
$1/2^-$	*S*-wave	*S*-wave
$3/2^+$	*S*-wave	*P*-wave
$3/2^-$	*S*-wave	*D*-wave
$5/2^+$	*P*-wave	*F*-wave
$5/2^-$	*P*-wave	*D*-wave

We then consider the quantum numbers of the $J/\psi\Lambda$ in the final state for fixed spin-parity of the $\Xi(2120)$. For the same reason mentioned before, the D- or higher partial wave interactions are not considered in the present discussion. If the quantum numbers of the $J/\psi\Lambda$ system are $1/2^+$ or $3/2^+$, the $\chi_{c1}\Lambda$ system can be in an S-wave and the $J/\psi\Lambda$ in a P-wave. On the contrary, if the quantum numbers of the $J/\psi\Lambda$ system are $1/2^-$ or $3/2^-$, there is a P-wave in the $\chi_{c1}\Lambda$ system and an S-wave in the $J/\psi\Lambda$ system. In both cases, there are an S-wave and a P-wave for this four-particle-vertex, but the corresponding behaviors of these two triangle loop integrations are different. As discussed in the previous paragraph, the effective Lagrangian of a P-wave interaction is proportional to the relative momentum of the involved particle. Meanwhile, at the singularity point, the invariant mass $m_{J/\psi\Lambda}$ is not far away from the $\chi_{c1}\Lambda$ threshold, and both the χ_{c1} and the Λ are on-mass-shell. It tells that the momenta of the χ_{c1} and Λ are small. Thus, for the negative parity case, the P-wave is in the $\chi_{c1}\Lambda$ system, which provides a loop momentum q to the loop integral and suppresses the singular behavior around the $\chi_{c1}\Lambda$ threshold, while the P-wave interaction of the $J/\psi\Lambda$ system for the positive parity case is independent of the loop integration. In the next step, we will take the quantum numbers of the $J/\psi\Lambda$ system as $1/2^+$ and $1/2^-$, respectively, to investigate how the finial results are affected.

We first take the quantum numbers of the $J/\psi\Lambda$ system being $1/2^+$ and the spin-parity of the $\Xi(2120)$ are assumed to be $1/2^-$. The amplitudes for the vertices are constructed as

$$
\begin{aligned}
t_{\Xi_b\Xi^*\chi_{c1}} &= g_a\bar{u}(P-q)\gamma^\mu u(P)\epsilon_\mu^*(q), \\
t_{\Xi^*\Lambda\bar{K}} &= g_b\bar{u}(k_1-q)u(P-q), \\
t_{\Lambda\chi_{c1}\Lambda J/\psi} &= g_c\epsilon_\mu(q)\bar{u}(k_1-k_2)\left(\slashed{k}_1+\sqrt{k_1^2}\right)\gamma_5\left(\gamma^\mu-\frac{k_1^\mu\slashed{k}_1}{k_1^2}\right)u(k_1-q)\epsilon_\nu^*(k_2)k_1^\nu\frac{k_1^2+m_{J/\psi}^2-m_\Lambda^2}{k_1^2},
\end{aligned}
$$

(2)

here we follow the momentum conventions given in Figure 1a. The amplitude of this triangle diagram reads

$$\mathcal{M} = g \int \frac{d^4 q}{(2\pi)^4} \bar{u}(k_1 - k_2) \left(\slashed{k}_1 + \sqrt{k_1^2} \right) \gamma_5 \left(\gamma^\mu - \frac{k_1^\mu \slashed{k}_1}{k_1^2} \right) \frac{\slashed{k}_1 - \slashed{q} + m_3}{(k_1 - q)^2 - m_3^2} \frac{\slashed{P} - \slashed{q} + m_2}{(P - q)^2 - m_2^2 + im_2\Gamma_2}$$

$$\times \frac{-\gamma_\mu + \frac{q_\mu \slashed{q}}{m_1^2}}{q^2 - m_1^2 + im_1\Gamma_1} u(P) \frac{k_1^2 + m_{J/\psi}^2 - m_\Lambda^2}{k_1^2} \epsilon_\nu^*(k_2) k_1^\nu. \tag{3}$$

Then we calculate the decay with the quantum numbers of the $J/\psi\Lambda$ system being $1/2^-$. The amplitude for the $\Lambda \chi_{c1} \Lambda J/\psi$ vertex reads

$$t_{\Lambda\chi_{c1}\Lambda J/\psi} = g_c \bar{u}(k_1 - k_2)\gamma_5 \left(\gamma^\mu - \frac{k_1^\mu \slashed{k}_1}{k_1^2} \right) \left(\slashed{k}_1 + \sqrt{k_1^2} \right) u(k_1 - q) \epsilon_\mu^*(k_2) \epsilon_\nu(q) k_1^\nu \frac{2k_1 \cdot q}{k_1^2}, \tag{4}$$

and the amplitude in this case is

$$\mathcal{M} = g \int \frac{d^4 q}{(2\pi)^4} \bar{u}(k_1 - k_2)\gamma_5 \left(\gamma^\mu - \frac{k_1^\mu \slashed{k}_1}{k_1^2} \right) \left(\slashed{k}_1 + \sqrt{k_1^2} \right) \frac{\slashed{k}_1 - \slashed{q} + m_3}{(k_1 - q)^2 - m_3^2} \frac{\slashed{P} - \slashed{q} + m_2}{(P - q)^2 - m_2^2 + im_2\Gamma_2}$$

$$\times \frac{-\slashed{k}_1 + \frac{\slashed{q}}{m_1^2} k_1 \cdot q}{q^2 - m_1^2 + im_1\Gamma_1} u(P) \frac{2k_1 \cdot q}{k_1^2} \epsilon_\mu^*(k_2). \tag{5}$$

It should be noticed that the absolute values of the coupling constants in both cases are unknown. Therefore, our results are normalized to 1 at the maximum. The differential decay width in the rest frame of the initial particle Ξ_b is

$$d\Gamma = \frac{1}{(2\pi)^3} \frac{1}{32 m_{\Xi_b}^3} \overline{|\mathcal{M}|^2} dm_{K\Lambda}^2 dm_{J/\psi\Lambda}^2. \tag{6}$$

After integrating $dm_{K\Lambda}^2$, the normalized differential decay widths in the $J/\psi\Lambda$ invariant mass distribution in these two cases are shown in Figure 3 with the widths of the exchanged particles taken into consideration.
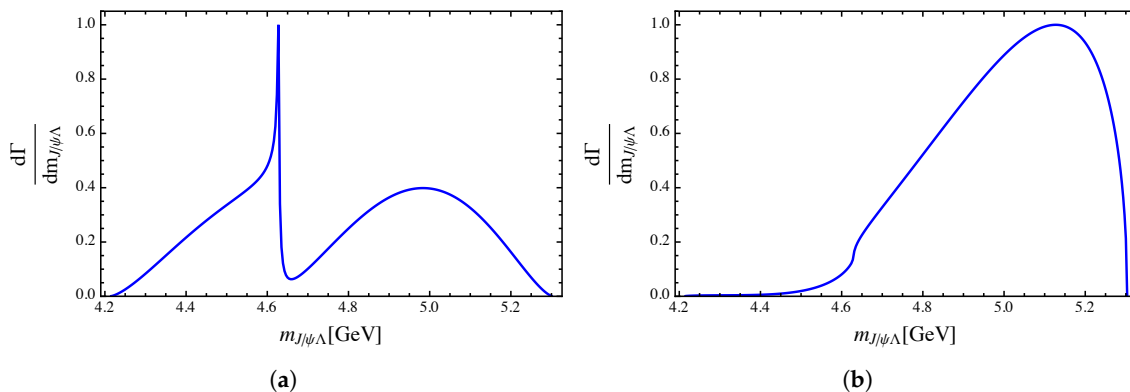
Figure 3. The $m_{J/\psi\Lambda}$ invariant mass distribution for the $\Xi_b^- \to K^- J/\psi\Lambda$ process via the $\chi_{c1}\Xi(2120)\Lambda$ loop with the quantum numbers of the $J/\psi\Lambda$ system being (**a**) $1/2^+$, and (**b**) $1/2^-$, respectively.

It can be seen that in the $1/2^+$ case the peak structure from the triangle singularity emerges at $m_{J/\psi\Lambda} = 4.628$ GeV and is distinct enough comparing to the background. However, this structure could not be observed any more in the $1/2^-$ case. Naively one would expect that the peak should still be there since the numerator of the integral would not diminish the singularity generated from the denominator.

Then here arises a question why the *P*-wave $\chi_{c1}\Lambda$ in the four-particle vertex can suppress the singular behavior so much. When constructing the effective Lagrangian of the four-particle vertex in the Lorentz covariant orbital-spin coupling scheme [73], the *P*-wave interaction in the $\chi_{c1}\Lambda$ system introduces a factor of the momentum difference of the exchanged Λ and χ_{c1}. Thus, the amplitude is directly proportional to the velocity difference between these two particles in the $1/2^-$ case. As discussed above, when the triangle singularity happens, all the three intermediate particles are on the mass shell and the process of each vertex actually happens classically. In this $\chi_{c1}\Xi(2120)\Lambda$ loop diagram, we find that the velocity of the intermediate Λ is very close to that of the χ_{c1} when the singularity occurs. In other words, their relative velocity is quite small in the rest frame of Ξ_b, meaning that the singularity is located very close to the $\chi_{c1}\Lambda$ threshold. More specifically, the factor $\left(-\not{k}_1 + \frac{\not{q}}{m_1^2} k_1 \cdot q\right)$ in Equation (5) from the *P*-wave $\chi_{c1}\Lambda$ system in the triangle singularity region can be derived as follows,

$$ -\not{k}_1 + \frac{\not{q}}{m_1^2} k_1 \cdot q \sim \frac{|\vec{q}|}{q^0} - \frac{|\vec{k}_1|}{k_1^0} \sim v_\Lambda - v_{\chi_{c1}} \sim 0, \tag{7} $$

explaining the suppression of the singular behavior in this case.

Since the amplitude is actually related to the partial wave interactions of the $\chi_{c1}\Lambda \to J/\psi\Lambda$ vertex, the $3/2^+$ and $3/2^-$ cases should be similar to the $1/2^+$ and $1/2^-$ cases, respectively. This indicates that this $\Xi(2120)\chi_{c1}\Lambda$ loop diagram could generate a peak in the $m_{J/\psi\Lambda}$ mass spectrum for the $\Xi_b^- \to K^- J/\psi\Lambda$ decay when the quantum numbers of the $J/\psi\Lambda$ system are $1/2^+$ or $3/2^+$. We then note that the threshold of the $\chi_{c1}\Lambda$ is at 4.626 GeV, which gives rise to a cusp (for the *S*-wave) in the distribution of the differential decay width. As the positions of the threshold and the triangle singularity (at about 4.628 GeV) are quite close, these two structures would lead to only one peak around this energy as shown in Figure 3a. Thus, if a structure is observed in this region in future experiments, the triangle singularity effects need to be taken into account for the $J^P = \frac{1}{2}^+$ or $\frac{3}{2}^+$ quantum numbers.

There are a lot of similarities between the $\Lambda_b \to K^- J/\psi p$ and $\Xi_b \to K^- J/\psi\Lambda$ through triangle loop diagrams. The $\Lambda_b\Lambda^*\chi_{c1}$ vertex, as considered in Refs. [28,31], and the $\Xi_b\Xi^*\chi_{c1}$ vertex involve the same product of CKM matrix elements and should share a similar coupling. The strength of the two four-particle-vertices $\chi_{c1}p \to J/\psi p$ and $\chi_{c1}\Lambda \to J/\psi\Lambda$ should also be similar due to the approximate light-flavor SU(3) symmetry. For the two rest vertices $\Lambda(1890)K^- p$ and $\Xi(2120)K^-\Lambda$, the $\bar{K}N$ channel occupies a rate of 20–35% among all the decay modes of $\Lambda(1890)$, while the branching ratio of $\Xi(2120)$ is still unknown and $\bar{K}\Lambda$ is the only observed decay channel. We can roughly regard the strengths of these two vertices to be of the same order of magnitude. Thus, studying possible structures in the $\Xi_b \to K^- J/\psi\Lambda$ decay around 4.63 GeV should also provide useful insights into the possible role of triangle singularity in the $\Lambda_b \to K^- J/\psi p$ decay around 4.45 GeV. Yet, the existence of one-star $\Xi(2120)$ state needs to be confirmed, which can be studied by analyzing the $\Lambda\bar{K}$ invariant mass distribution of the process under discussion.

4. Summary

Inspired by the analysis of the triangle singularities in the $\Lambda_b \to K^- J/\psi p$ process in Ref. [31], we apply the same method to the $\Xi_b \to K^- J/\psi\Lambda$ process via charmonium-Ξ^*-Λ intermediate states to check whether there exist possible triangle singularities. We find that there are 11 and 7 possible triangle singularities with various combinations of charmonium-Ξ^* states and D_S^*-Ξ_c^* states, respectively. For the former, the $\chi_{c1}\Xi(2120)\Lambda$ loop diagram is expected to be the most promising process to observe the singularity structure; for the latter, those with $\bar{D}_{s1}^*(2700)$ listed in Table 2 should be more important than the others. Nevertheless, the absolute values of all these amplitudes could not be precisely evaluated without knowing the amplitudes for all the involved vertices. For the $\chi_{c1}\Xi(2120)\Lambda$ diagram, when the spin-parity quantum numbers of the $J/\psi\Lambda$ system are $1/2^+$ or $3/2^+$, the joint effects of the triangle singularity and the $\chi_{c1}\Lambda$ threshold would produce a narrow peak around 4.63 GeV in the

$J/\psi\Lambda$ invariant mass distribution. A study of such effects needs to be taken into account in the search of hidden-charm strange pentaquarks, and a study of the $\Xi_b \to K^- J/\psi\Lambda$ will also shed light on the role of triangle singularities in the $\Lambda_b \to K^- J/\psi p$ process.

Author Contributions: Conceptualization, C.-W.S.; validation, C.-W.S. and H.-J.J.; formal analysis, C.-W.S., F.-K.G. and J.-J.W.; writing—original draft preparation, C.-W.S.; writing—review and editing, C.-W.S., H.-J.J., F.-K.G. and J.-J.W. All authors have read and agreed to the published version of the manuscript.

Funding: This work is supported in part by the Fundamental Research Funds for the Central Universities, by the National Natural Science Foundation of China (NSFC) under Grants No. 11835015, No. 11947302 and No. 11961141012, by the Chinese Academy of Sciences (CAS) under Grants No. XDB34030303 and No. QYZDB-SSW-SYS013, by NSFC and the Deutsche Forschungsgemeinschaft (DFG) through the funds provided to the Sino-German Collaborative Research Center "Symmetries and the Emergence of Structure in QCD" (NSFC Grant No. 11621131001, DFG Grant No. CRC110), and by the CAS Center for Excellence in Particle Physics (CCEPP).

Acknowledgments: We are grateful to Eulogio Oset for a careful reading of our manuscript.

Conflicts of Interest: The authors declare no conflict of interest.

References

1. Wu, J.J.; Molina, R.; Oset, E.; Zou, B.S. Prediction of narrow N^* and Λ^* resonances with hidden charm above 4 GeV. *Phys. Rev. Lett.* **2010**, *105*, 232001. [CrossRef] [PubMed]
2. Aaij, R. Observation of $J/\psi p$ Resonances Consistent with Pentaquark States in $\Lambda_b^0 \to J/\psi K^- p$ Decays. *Phys. Rev. Lett.* **2015**, *115*, 072001. [CrossRef] [PubMed]
3. Aaij, R. Observation of a narrow pentaquark state, $P_c(4312)^+$, and of two-peak structure of the $P_c(4450)^+$. *Phys. Rev. Lett.* **2019**, *122*, 222001. [CrossRef] [PubMed]
4. Xiao, C.W.; Nieves, J.; Oset, E. Prediction of hidden charm strange molecular baryon states with heavy quark spin symmetry. *Phys. Lett.* **2019**, *B799*, 135051. [CrossRef]
5. Xiao, C.W.; Nieves, J.; Oset, E. Combining heavy quark spin and local hidden gauge symmetries in the dynamical generation of hidden charm baryons. *Phys. Rev.* **2013**, *D88*, 056012. [CrossRef]
6. Wang, B.; Meng, L.; Zhu, S.L. Spectrum of the strange hidden charm molecular pentaquarks in chiral effective field theory. *Phys. Rev.* **2020**, *D101*, 034018. [CrossRef]
7. Irie, Y.; Oka, M.; Yasui, S. Flavor-singlet hidden charm pentaquark. *Phys. Rev.* **2018**, *D97*, 034006. [CrossRef]
8. Chen, R.; He, J.; Liu, X. Possible strange hidden-charm pentaquarks from $\Sigma_c^{(*)}\bar{D}_s^*$ and $\Xi_c^{(',*)}\bar{D}^*$ interactions. *Chin. Phys.* **2017**, *C41*, 103105. [CrossRef]
9. Shen, C.W.; Wu, J.J.; Zou, B.S. Decay behaviors of possible $\Lambda_{c\bar{c}}$ states in hadronic molecule pictures. *Phys. Rev.* **2019**, *D100*, 056006. [CrossRef]
10. Lu, J.X.; Wang, E.; Xie, J.J.; Geng, L.S.; Oset, E. The $\Lambda_b \to J/\psi K^0\Lambda$ reaction and a hidden-charm pentaquark state with strangeness. *Phys. Rev.* **2016**, *D93*, 094009. [CrossRef]
11. Feijoo, A.; Magas, V.K.; Ramos, A.; Oset, E. A hidden-charm $S = -1$ pentaquark from the decay of Λ_b into $J/\psi, \eta\Lambda$ states. *Eur. Phys. J.* **2016**, *C76*, 446. [CrossRef]
12. Chen, H.X.; Geng, L.S.; Liang, W.H.; Oset, E.; Wang, E.; Xie, J.J. Looking for a hidden-charm pentaquark state with strangeness $S = -1$ from Ξ_b^- decay into $J/\psi K^-\Lambda$. *Phys. Rev.* **2016**, *C93*, 065203. [CrossRef]
13. Aaij, R. Observation of the $\Xi_b^- \to J/\psi\Lambda K^-$ decay. *Phys. Lett.* **2017**, *B772*, 265–273. [CrossRef]
14. Coleman, S.; Norton, R.E. Singularities in the physical region. *Nuovo Cim.* **1965**, *38*, 438–442. [CrossRef]
15. Karplus, R.; Sommerfield, C.M.; Wichmann, E.H. Spectral Representations in Perturbation Theory. 1. Vertex Function. *Phys. Rev.* **1958**, *111*, 1187–1190. [CrossRef]
16. Landau, L.D. On analytic properties of vertex parts in quantum field theory. *Nucl. Phys.* **1960**, *13*, 181–192. [CrossRef]
17. Bjorken, J.D. Experimental Tests of Quantum Electrodynamics and Spectral Representations of Green's Functions in Perturbation Theory. Ph.D. Thesis, Stanford University, Stanford, CA, USA, 1959.
18. Schmid, C. Final-State Interactions and the Simulation of Resonances. *Phys. Rev.* **1967**, *154*, 1363. [CrossRef]
19. Wu, J.J.; Liu, X.H.; Zhao, Q.; Zou, B.S. The Puzzle of anomalously large isospin violations in $\eta(1405/1475) \to 3\pi$. *Phys. Rev. Lett.* **2012**, *108*, 081803. [CrossRef]

20. Aceti, F.; Liang, W.H.; Oset, E.; Wu, J.J.; Zou, B.S. Isospin breaking and $f_0(980)$-$a_0(980)$ mixing in the $\eta(1405) \to \pi^0 f_0(980)$ reaction. *Phys. Rev.* **2012**, *D86*, 114007. [CrossRef]

21. Wu, X.G.; Wu, J.J.; Zhao, Q.; Zou, B.S. Understanding the property of $\eta(1405/1475)$ in the J/ψ radiative decay. *Phys. Rev.* **2013**, *D87*, 014023. [CrossRef]

22. Wang, Q.; Hanhart, C.; Zhao, Q. Decoding the riddle of $Y(4260)$ and $Z_c(3900)$. *Phys. Rev. Lett.* **2013**, *111*, 132003. [CrossRef] [PubMed]

23. Wang, Q.; Hanhart, C.; Zhao, Q. Systematic study of the singularity mechanism in heavy quarkonium decays. *Phys. Lett.* **2013**, *B725*, 106–110. [CrossRef]

24. Mikhasenko, M.; Ketzer, B.; Sarantsev, A. Nature of the $a_1(1420)$. *Phys. Rev.* **2015**, *D91*, 094015. [CrossRef]

25. Achasov, N.N.; Kozhevnikov, A.A.; Shestakov, G.N. Isospin breaking decay $\eta(1405) \to f_0(980)\pi^0 \to 3\pi$. *Phys. Rev.* **2015**, *D92*, 036003. [CrossRef]

26. Liu, X.H.; Oka, M.; Zhao, Q. Searching for observable effects induced by anomalous triangle singularities. *Phys. Lett.* **2016**, *B753*, 297–302. [CrossRef]

27. Liu, X.H.; Wang, Q.; Zhao, Q. Understanding the newly observed heavy pentaquark candidates. *Phys. Lett.* **2016**, *B757*, 231–236. [CrossRef]

28. Guo, F.K.; Meißner, U.G.; Wang, W.; Yang, Z. How to reveal the exotic nature of the P$_c$(4450). *Phys. Rev.* **2015**, *D92*, 071502. [CrossRef]

29. Szczepaniak, A.P. Triangle Singularities and XYZ Quarkonium Peaks. *Phys. Lett.* **2015**, *B747*, 410–416. [CrossRef]

30. Guo, F.K.; Meißner, U.G.; Nieves, J.; Yang, Z. Remarks on the P_c structures and triangle singularities. *Eur. Phys. J.* **2016**, *A52*, 318. [CrossRef]

31. Bayar, M.; Aceti, F.; Guo, F.K.; Oset, E. A Discussion on Triangle Singularities in the $\Lambda_b \to J/\psi K^- p$ Reaction. *Phys. Rev.* **2016**, *D94*, 074039. [CrossRef]

32. Wang, E.; Xie, J.J.; Liang, W.H.; Guo, F.K.; Oset, E. Role of a triangle singularity in the $\gamma p \to K^+ \Lambda(1405)$ reaction. *Phys. Rev.* **2017**, *C95*, 015205. [CrossRef]

33. Pilloni, A.; Fernandez-Ramirez, C.; Jackura, A.; Mathieu, V.; Mikhasenko, M.; Nys, J.; Szczepaniak, A. Amplitude analysis and the nature of the Z$_c$(3900). *Phys. Lett. B* **2017**, *772*, 200–209. [CrossRef]

34. Xie, J.J.; Geng, L.S.; Oset, E. $f_2(1810)$ as a triangle singularity. *Phys. Rev.* **2017**, *D95*, 034004. [CrossRef]

35. Szczepaniak, A.P. Dalitz plot distributions in presence of triangle singularities. *Phys. Lett.* **2016**, *B757*, 61–64. [CrossRef]

36. Roca, L.; Oset, E. Role of a triangle singularity in the $\pi\Delta$ decay of the $N(1700)(3/2^-)$. *Phys. Rev.* **2017**, *C95*, 065211. [CrossRef]

37. Debastiani, V.R.; Sakai, S.; Oset, E. Role of a triangle singularity in the $\pi N(1535)$ contribution to $\gamma p \to p\pi^0\eta$. *Phys. Rev.* **2017**, *C96*, 025201. [CrossRef]

38. Samart, D.; Liang, W.; Oset, E. Triangle mechanisms in the build up and decay of the $N^*(1875)$. *Phys. Rev.* **2017**, *C96*, 035202. [CrossRef]

39. Sakai, S.; Oset, E.; Ramos, A. Triangle singularities in $B^- \to K^- \pi^- D_{s0}^+$ and $B^- \to K^- \pi^- D_{s1}^+$. *Eur. Phys. J.* **2018**, *A54*, 10. [CrossRef]

40. Pavao, R.; Sakai, S.; Oset, E. Triangle singularities in $B^- \to D^{*0}\pi^-\pi^0\eta$ and $B^- \to D^{*0}\pi^-\pi^+\pi^-$. *Eur. Phys. J.* **2017**, *C77*, 599. [CrossRef]

41. Xie, J.J.; Guo, F.K. Triangular singularity and a possible ϕp resonance in the $\Lambda_c^+ \to \pi^0 \phi p$ decay. *Phys. Lett.* **2017**, *B774*, 108–113. [CrossRef]

42. Bayar, M.; Pavao, R.; Sakai, S.; Oset, E. Role of the triangle singularity in $\Lambda(1405)$ production in the $\pi^- p \to K^0 \pi\Sigma$ and $pp \to pK^+ \pi\Sigma$ processes. *Phys. Rev.* **2018**, *C97*, 035203. [CrossRef]

43. Liang, W.H.; Sakai, S.; Xie, J.J.; Oset, E. Triangle singularity enhancing isospin violation in $\bar{B}_s^0 \to J/\psi\pi^0 f_0(980)$. *Chin. Phys.* **2018**, *C42*, 044101. [CrossRef]

44. Oset, E.; Roca, L. Triangle singularity in $\tau \to f_1(1285)\pi\nu_\tau$ decay. *Phys. Lett.* **2018**, *B782*, 332–338. [CrossRef]

45. Dai, L.R.; Pavao, R.; Sakai, S.; Oset, E. Anomalous enhancement of the isospin-violating $\Lambda(1405)$ production by a triangle singularity in $\Lambda_c \to \pi^+\pi^0\pi^0\Sigma^0$. *Phys. Rev.* **2018**, *D97*, 116004. [CrossRef]

46. Dai, L.R.; Yu, Q.X.; Oset, E. Triangle singularity in $\tau^- \to \nu_\tau \pi^- f_0(980)$ $(a_0(980))$ decays. *Phys. Rev.* **2019**, *D99*, 016021. [CrossRef]

47. Guo, F.K. Novel Method for Precisely Measuring the $X(3872)$ Mass. *Phys. Rev. Lett.* **2019**, *122*, 202002. [CrossRef]

48. Liang, W.H.; Chen, H.X.; Oset, E.; Wang, E. Triangle singularity in the $J/\psi \to K^+K^- f_0(980)(a_0(980))$ decays. *Eur. Phys. J.* **2019**, *C79*, 411. [CrossRef]

49. Nakamura, S.X. Triangle singularities in $\bar{B}^0 \to \chi_{c1} K^- \pi^+$ relevant to $Z_1(4050)$ and $Z_2(4250)$. *Phys. Rev.* **2019**, *D100*, 011504. [CrossRef]

50. Du, M.C.; Zhao, Q. Internal particle width effects on the triangle singularity mechanism in the study of the $\eta(1405)$ and $\eta(1475)$ puzzle. *Phys. Rev.* **2019**, *D100*, 036005. [CrossRef]

51. Liu, X.H.; Li, G.; Xie, J.J.; Zhao, Q. Visible narrow cusp structure in $\Lambda_c^+ \to pK^-\pi^+$ enhanced by triangle singularity. *Phys. Rev.* **2019**, *D100*, 054006. [CrossRef]

52. Jing, H.J.; Sakai, S.; Guo, F.K.; Zou, B.S. Triangle singularities in $J/\psi \to \eta\pi^0\phi$ and $\pi^0\pi^0\phi$. *Phys. Rev.* **2019**, *D100*, 114010. [CrossRef]

53. Braaten, E.; He, L.P.; Ingles, K. Triangle Singularity in the Production of X(3872) and a Photon in e^+e^- Annihilation. *Phys. Rev.* **2019**, *D100*, 031501. [CrossRef]

54. Sakai, S.; Oset, E.; Guo, F.K. Triangle singularity in the $B^- \to K^-\pi^0 X(3872)$ reaction and sensitivity to the X(3872) mass. *Phys. Rev.* **2020**, *D101*, 054030. [CrossRef]

55. Sakai, S. Role of the triangle mechanism in the $\Lambda_b \to \Lambda_c \pi^- f_0(980)$ reaction. *Phys. Rev.* **2020**, *D101*, 074041. [CrossRef]

56. Molina, R.; Oset, E. Triangle singularity in $B^- \to K^- X(3872); X \to \pi^0\pi^+\pi^-$ and the X(3872) mass. *Eur. Phys. J.* **2020**, *C80*, 451. [CrossRef]

57. Braaten, E.; He, L.P.; Ingles, K.; Jiang, J. Charm-meson triangle singularity in e^+e^- annihilation into $D^{*0}\bar{D}^0 + \gamma$. *Phys. Rev. D* **2020**, *101*, 096020. [CrossRef]

58. Alexeev, M.G.; Alexeev, G.D.; Amoroso, A.; Andrieux, V.; Anosov, V.; Antoshkin, A.; Augsten, K.; Augustyniak, W.; Azevedo, C.D.R.; Badelek, B.; et al. A Triangle Singularity as the Origin of the $a_1(1420)$. *arXiv* **2020**, arXiv:2006.05342.

59. Ortega, P.G.; Ruiz Arriola, E. On the precise measurement of the X(3872) mass and its counting rate. *arXiv* **2020**, arXiv:2007.11608.

60. Guo, F.K.; Liu, X.H.; Sakai, S. Threshold cusps and triangle singularities in hadronic reactions. *Prog. Part. Nucl. Phys.* **2020**, *112*, 103757. [CrossRef]

61. Sakai, S.; Jing, H.J.; Guo, F.K. Decays of P_c into $J/\psi N$ and $\eta_c N$ with heavy quark spin symmetry. *Phys. Rev. D* **2019**, *100*, 074007. [CrossRef]

62. Chen, H.X.; Chen, W.; Liu, X.; Steele, T.G.; Zhu, S.L. Towards exotic hidden-charm pentaquarks in QCD. *Phys. Rev. Lett.* **2015**, *115*, 172001. [CrossRef] [PubMed]

63. Roca, L.; Nieves, J.; Oset, E. LHCb pentaquark as a $\bar{D}^*\Sigma_c - \bar{D}^*\Sigma_c^*$ molecular state. *Phys. Rev.* **2015**, *D92*, 094003. [CrossRef]

64. He, J. $\bar{D}\Sigma_c^*$ and $\bar{D}^*\Sigma_c$ interactions and the LHCb hidden-charmed pentaquarks. *Phys. Lett.* **2016**, *B753*, 547–551. [CrossRef]

65. Lin, Y.H.; Shen, C.W.; Guo, F.K.; Zou, B.S. Decay behaviors of the P_c hadronic molecules. *Phys. Rev.* **2017**, *D95*, 114017. [CrossRef]

66. He, J. Understanding spin parity of $P_c(4450)$ and $Y(4274)$ in a hadronic molecular state picture. *Phys. Rev.* **2017**, *D95*, 074004. [CrossRef]

67. Chen, H.X.; Cui, E.L.; Chen, W.; Liu, X.; Steele, T.G.; Zhu, S.L. QCD sum rule study of hidden-charm pentaquarks. *Eur. Phys. J.* **2016**, *C76*, 572. [CrossRef]

68. Xiang, J.B.; Chen, H.X.; Chen, W.; Li, X.B.; Yao, X.Q.; Zhu, S.L. Revisiting hidden-charm pentaquarks from QCD sum rules. *Chin. Phys.* **2019**, *C43*, 034104. [CrossRef]

69. Zyla, P.A.; Barnett, R.M.; Beringer, J.; Dahl, O.; Dwyer, D.A.; Groom, D.E.; Lin, C.-J.; Lugovsky, K.S.; Pianori, E.; Robinson, D.J.; et al. Review of Particle Physics. *Prog. Theor. Exp. Phys.* **2020**, *2020*, 083C01. [CrossRef]

70. Brodzicka, J. Observation of a new D_{sJ} meson in $B^+ \to \bar{D}^0 D^0 K^+$ decays. *Phys. Rev. Lett.* **2008**, *100*, 092001. [CrossRef]

71. Lees, J. Dalitz plot analyses of $B^0 \to D^-D^0 K^+$ and $B^+ \to \bar{D}^0 D^0 K^+$ decays. *Phys. Rev. D* **2015**, *91*, 052002. [CrossRef]

72. Aaij, R.; De Cian, M.; De Miranda, J.M.; De Paula, L.; De Silva, W. Observation of overlapping spin-1 and spin-3 $\bar{D}^0 K^-$ resonances at mass 2.86 GeV/c^2. *Phys. Rev. Lett.* **2014**, *113*, 162001. [CrossRef] [PubMed]

73. Zou, B.S.; Hussain, F. Covariant L-S scheme for the effective N*NM couplings. *Phys. Rev.* **2003**, *C67*, 015204. [CrossRef]

74. Alitti, J.; Barnes, V.E.; Flaminio, E.; Metzger, W.; Radojičić, D.; Rau, R.R.; Richardson, C.R.; Samios, N.P.; Bassano, D.; Goldberg, M.; et al. Strangeness $S = -2$ baryon resonance. *Phys. Rev. Lett.* **1969**, *22*, 79–82. [CrossRef]

75. Hemingway, R.J.; Armenteros, R.; Berge, J.P.; Diaz, J.; Gay, J.B.; Trepagnier, P.; Jongejans, B.; Massaro, G.G.G.; Voorthuis, H.; Heinen, P.M.; et al. Xi* (2030) Production in K^- p Reactions at 4.2-GeV/c. *Phys. Lett.* **1977**, *68B*, 197. [CrossRef]

76. Bartsch, J.; Bartsch, J.; Deutschmann, M.; Hermanns, M.; Keppel, E.; Speth, R.; Gensch, U.; Grote, C.; Pose, D.; Schiller, H.; et al. Evidence for a new xi resonance at 2500 mev in 10 gev/c k-minus p interactions. *Phys. Lett.* **1969**, *28B*, 439–442. [CrossRef]